

Determination and Combination of Monthly Gravity Field Time Series from Kinematic Orbits of GRACE, GRACE-FO and Swarm

Thomas Grombein, Martin Lasser, Daniel Arnold, Ulrich Meyer, and Adrian Jäggi

Abstract

Dedicated gravity field missions like GRACE and GRACE-FO use ultra-precise inter-satellite ranging observations to derive time series of monthly gravity field solutions. In addition, any (non-dedicated) Low Earth Orbiting (LEO) satellite with a dual-frequency GNSS receiver may also serve as a gravity field sensor. To this end, GPS-derived kinematic LEO orbit positions are used as pseudo-observations for gravity field recovery. Although less sensitive, this technique can provide valuable information for the monitoring of large-scale time-variable gravity signals, particularly for those months where no inter-satellite ranging measurements are available. Due to a growing number of LEO satellites that collect continuous and mostly uninterrupted GPS data, the value of a combined multi-LEO gravity field time series is likely to increase in the near future.

In this paper, we present monthly gravity field time series derived from GPS-based kinematic orbit positions of the GRACE, GRACE-FO and Swarm missions. We analyze their individual contribution as well as the additional benefit of their combination. For this purpose, two combination strategies at solution level are studied that are based on (i) least-squares variance component estimation, and (ii) stochastic properties of the gravity field solutions. By evaluating mass variations in Greenland and the Amazon river basin, the resulting gravity field time series are assessed with respect to superior solutions based on inter-satellite ranging.

Keywords

GPS-based gravity field recovery · GRACE · GRACE-FO · Gravity field combination · Kinematic orbits · LEO satellites · Swarm · Time-variable gravity

1 Introduction

The Earth's gravity field and its temporal variations provide an important source of information for the monitoring of mass transport and mass distribution in the Earth's system. Dedicated satellite missions like the Gravity Recovery And Climate Experiment (GRACE, Tapley et al. 2004) and its successor GRACE Follow-On (GRACE-FO,

Landerer et al. 2020) allow to resolve the Earth's time-variable gravity field on a monthly basis using ultra-precise inter-satellite ranging derived from K-band or laser ranging data.

Alternative gravity field information can be obtained from Low Earth Orbiting (LEO) satellites that are equipped with a high-quality (geodetic) GNSS receiver. For this purpose, GPS tracking data may be used to derive precise kinematic orbits (Švehla and Rothacher 2005). As kinematic orbit positions are purely geometrically determined and independent of the LEO orbital dynamics, they are well suited for gravity field recovery. Several methods have been proposed

T. Grombein (✉) · M. Lasser · D. Arnold · U. Meyer · A. Jäggi
Astronomical Institute, University of Bern, Bern, Switzerland
e-mail: thomas.grombein@aiub.unibe.ch

to derive gravity field information from kinematic LEO orbit positions, see, e.g., Baur et al. (2014) for a detailed overview.

Many studies have demonstrated that it is feasible to recover large-scale time-variable gravity field signals from kinematic LEO orbits, see, e.g., Weigelt et al. (2013), Guo et al. (2020) and Grombein et al. (2021) for studies related to the dedicated gravity field missions CHAMP, GRACE and GOCE, respectively. In recent years, time-variable gravity information derived from GPS tracking data of the (non-dedicated) magnetic field mission Swarm (Friis-Christensen et al. 2008) moved into focus to bridge the gap between the GRACE and GRACE-FO missions, see, e.g., Richter et al. (2021). Moreover, monthly gravity field solutions from Swarm kinematic orbits are computed by different institutes and operationally combined (Teixeira da Encarnação et al. 2020) in the frame of the International Combination Service for Time-variable Gravity Fields (COST-G, Jäggi et al. 2020).

Beside such a single-mission combination, the increasing number of operational scientific LEO satellites and commercial satellite constellations makes it attractive to strive for a combined GPS-based gravity field time series derived from multiple LEO satellites. Such a combination will take advantage of (i) a large number of mostly uninterrupted observations, and (ii) the variety of complementary orbital configurations that can improve the spatio-temporal resolution. Moreover, such a multi-LEO combination might play an important role for a continuation of gravity field time series when no dedicated mission is in orbit, e.g., due to a potential failure of GRACE-FO or a large gap until the next generation gravity field mission (NGGM) is launched.

At the Astronomical Institute of the University of Bern (AIUB), GPS-based precise orbit determination (POD) is routinely performed for a variety of LEO satellite using the POD strategy described in Jäggi et al. (2006) that is implemented in the Bernese GNSS Software (Dach et al. 2015). Kinematic orbits are processed in 24 h orbital arcs in a batch least-squares adjustment using the ionosphere-free linear combination of the undifferenced GPS carrier phase observations. For this purpose, the final CODE GNSS orbits (Dach et al. 2009) and 5 s satellite clock corrections (Bock et al. 2009) are used. Furthermore, for each LEO GPS receiver antenna, in-flight calibrated phase center variation maps are generated by a residual stacking approach (Jäggi et al. 2009). Beside conventional ambiguity-float orbits, also ambiguity-fixed orbits are recently being computed based on new phase bias and clock products (Schaer et al. 2021). Kinematic orbits have been generated for various LEO satellites like CHAMP, GRACE and GOCE or are routinely processed for a growing number of operational missions like GRACE-FO and Swarm or the fleet of Sentinel satellites. This offers the opportunity to explore the contribution of these kinematic orbits to the recovery of the Earth's time-variable gravity field.

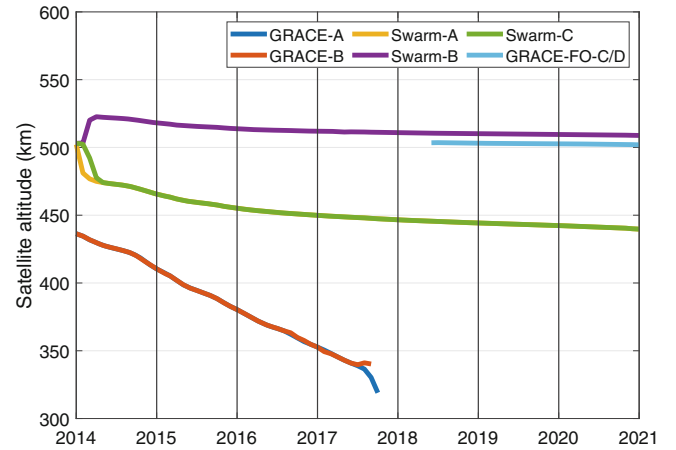


Fig. 1 Orbital altitudes of the GRACE, GRACE-FO and Swarm satellites derived from their kinematic orbit positions (monthly mean values)

In the present study, we use the kinematic LEO orbit positions from the dedicated satellite missions GRACE and GRACE-FO as well as from the non-dedicated Swarm constellation in order to determine and combine monthly gravity field time series covering about seven years between Jan 2014 and Feb 2021. As illustrated in Fig. 1, the orbital altitudes of these LEO satellites are quite different. This certainly represents a major difference to the setting of combinations performed within COST-G. Therefore, it needs to be analyzed if classical combination schemes based on variance component estimation (VCE) as applied by COST-G can be adapted for this scenario.

The paper is organized as follows: in Sect. 2 details about the input data and gravity field recovery are provided. While the quality of the derived gravity field time series is analyzed in Sect. 3, two strategies for a combination at solution level are introduced and applied in Sect. 4. By evaluating time-variable gravity field signals in Greenland and the Amazon river basin, Sect. 5 studies the individual contribution of the time series and the additional value of their combination. Finally, Sect. 6 concludes with a summary and an outlook.

2 Gravity Field Recovery

The monthly GPS-based LEO gravity field time series presented in this study are generated with the Celestial Mechanics Approach (CMA, Beutler et al. 2010) as it is implemented in a development version of the Bernese GNSS Software. Following the procedure described in Jäggi et al. (2016), the GPS-derived kinematic LEO orbit positions and their epoch-wise covariance information are used as pseudo-observations to perform gravity field recovery in a generalized orbit determination problem, where arc-specific orbit and gravity field

Table 1 Overview and processing details of GPS-based gravity field time series for different LEO satellites

LEO satellites	GRACE-A/B	GRACE-FO-C/D	Swarm-A/B/C
Processing period	Jan 2014 – Oct 2017	Jun 2018 – Feb 2021	Jan 2014 – Feb 2021
Kinematic orbit type	Ambiguity-float	Ambiguity-fixed	Ambiguity-float/-fixed ^a
Data sampling	10 s	10 s	10 s / 5 s ^b
Accelerometer data	Used	Used	Not used
Initial conditions	6 orbital elements (daily)		6 orbital elements (daily)
Empirical parameters	—		Constant accelerations (daily)
Stochastic parameters	PCA ^c (15 min, 10 nm s ⁻² constr.)		PCA ^c (15 min, 10 / 7.07 nm s ⁻² constr. ^b)
Accelerometer parameters	Bias + scaling factors (daily)		—
Gravity field coefficients	Degree and order 90 (monthly)		Degree and order 70 (monthly)
Reference	This paper		Dahle et al. (2017)

^aSince 2020-01-26 ^b Since 2014-07-15 ^c PCA: Piecewise constant accelerations

parameters are estimated simultaneously. Non-gravitational forces are not explicitly modeled but considered by measured accelerometer data and/or absorbed by arc-specific empirical acceleration (e.g., constant, once- or twice-per-revolution). Remaining deficiencies are compensated by constrained stochastic parameters (e.g., pulses or piecewise constant accelerations), see Jäggi et al. (2006). Daily normal equations (NEQs) are set up and orbit parameters are pre-eliminated. These NEQs are then stacked month-wise and inverted to solve for monthly gravity field coefficients.

Table 1 provides details on the input data and the conducted gravity field processing for the different LEO satellites. We make use of our in-house generated GPS-based kinematic orbit products for GRACE-A/B (Arnold and Jäggi 2020a), GRACE-FO-C/D (Arnold and Jäggi 2020b), and Swarm-A/B/C (Arnold and Jäggi 2021) that are publicly available.¹ The GRACE/-FO kinematic orbit positions have a data sampling rate of 10 s. While this is also the case for the first months of Swarm, orbits starting from Jul 2014 feature an increased sampling rate of 1 s. For gravity field recovery, a downsampling to 5 s is used as a compromise of runtime reduction and required accuracy (comparisons show that differences are mainly restricted to the high frequency noise). Moreover, the kinematic Swarm positions are based on screened GPS measurements to mitigate ionosphere-induced disturbances affecting the orbit and gravity field quality (e.g., Dahle et al. 2017).

For gravity field recovery, the following parameters are used: beside the six daily orbital elements, stochastic parameters in terms of piecewise constant accelerations (PCA) are estimated in radial, along-track and cross-track direction at intervals of 15 min, using constraints as specified in Table 1 (intervals and constraints are empirically determined and found to be suitable in many studies with the CMA). To maintain an equal influence of the PCAs, the constraints for Swarm need to be reduced by a factor of $\sqrt{2}$ in Jul

2014 to account for the doubling of the sampling rate. In the GRACE/-FO processing, accelerometer measurements are taken into account whenever available, by co-estimating additional accelerometer bias and scaling factors. Moreover, in the case of the Swarm gravity field recovery, daily constant accelerations are estimated, which is implicitly also the case for GRACE/-FO due to the used accelerometer biases. Finally, gravity field parameters in terms of spherical harmonic (SH) coefficients up to degree and order (d/o) 90 (GRACE/-FO) and 70 (Swarm) are determined without applying any regularization.

It should be noted that the used maximum degree is far above the expected signal content and sensitivity of the GPS observations. However, this choice is motivated to (i) prevent that an omission error propagates into the low-degree coefficients (Guo et al. 2020), and to (ii) guarantee that the estimated SH coefficients are not biased towards the used a priori gravity field model due to an inconsistent maximum degree (Meyer et al. 2015).

While the gravity field recovery for GRACE/-FO has been conducted within this study, the monthly Swarm gravity fields are the operational AIUB solutions (Dahle et al. 2017) that contribute to the Swarm COST-G combination. In the considered time period between Jan 2014 and Feb 2021, the gravity field time series recovered from the kinematic orbits of GRACE, GRACE-FO and Swarm consist of 46, 33 and 86 monthly solutions, respectively. For each mission, combined as well as individual satellite time series have been generated. All monthly solutions are independent from each other as no temporal filtering is applied as, e.g., done in Weigelt et al. (2013) and Zhong et al. (2021).

3 Characteristics of Gravity Field Time Series

In order to analyze the quality of the GPS-based LEO gravity field time series, Fig. 2 shows difference degree amplitudes in terms of geoid heights with respect to the monthly ITSG-

¹http://www.aiub.unibe.ch/download/LEO_ORBITS

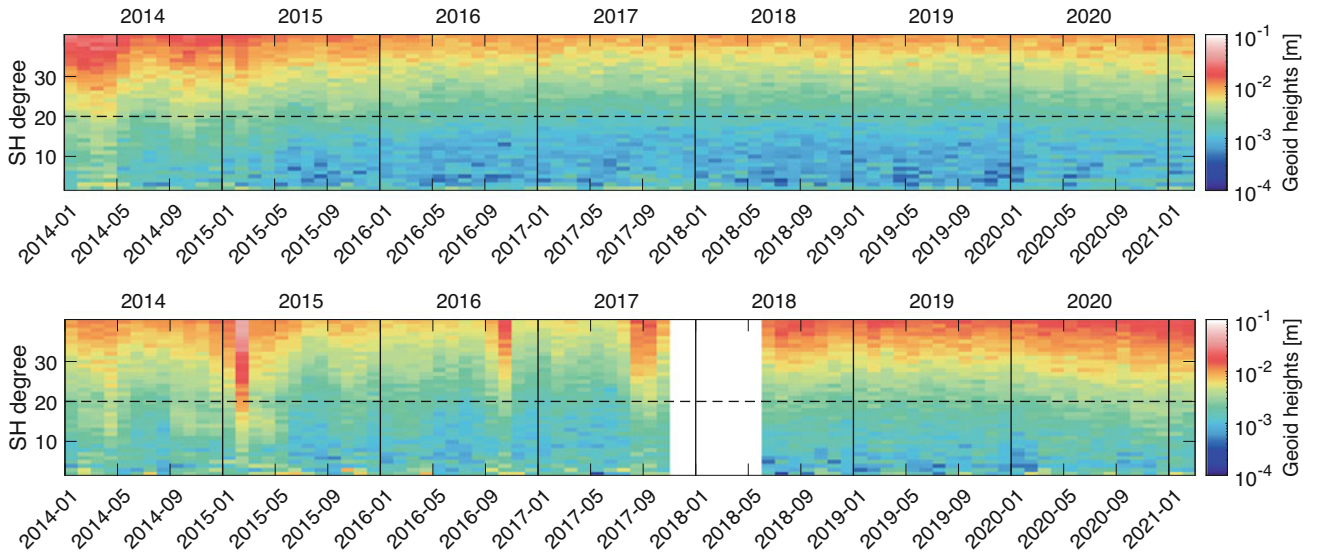


Fig. 2 Difference degree amplitudes (degree 2 to 40) in terms of geoid heights with respect to monthly ITSG-Grace2018 solutions for the GPS-based gravity field time series of GRACE (*top left*), GRACE-FO (*top*

right), and Swarm (*bottom*) in the time span Jan 2014 – Feb 2021. Note that gaps in the monthly ITSG-Grace2018 solutions are filled by interpolation.

Grace2018 solutions based on superior GRACE/-FO K-band data (Kvas et al. 2019). For the analysis in this section, gaps in the ITSG-Grace2018 time series are filled using interpolation at the epochs of the GPS-based solutions. Difference degree amplitudes shown in Fig. 2 are confined to degrees up to 40 in order to focus on the relevant signal content of the GPS-based gravity field solutions.

In the case of GRACE (Fig. 2, top left), the difference degree amplitudes generally exhibit values at the mm-level. However, the time series is apparently affected by several disturbances. For the lower degrees, seasonal variations in the difference degree amplitudes are visible, particularly in the years 2014 and 2015. Here, the GRACE solutions in spring and autumn systematically show larger differences for degrees up to 20–30. This systemic behavior can be associated with the ionospheric activity. As described in Sect. 2, a ionospheric-induced degradation of GPS-based gravity fields has been reported for Swarm (Dahle et al. 2017) and GOCE (Jäggi et al. 2015), but can also be observed for GRACE in this study. This is confirmed by Fig. 3, where geoid height differences for the GPS-based GRACE gravity fields of Aug 2014 and Apr 2015 are plotted in the space domain. In contrast to the unaffected month Aug 2014, the solution for Apr 2015 reveals typical signatures of ionospheric-induced artifacts in two bands along the geomagnetic equator. Starting from mid-2015, the quality of the GRACE monthly gravity field solutions gradually improved due to (i) a period of lower ionospheric activity, and (ii) the rapidly decreasing orbital altitudes of the GRACE satellites (cf. Fig. 1).

Besides seasonal disturbances, prominent discrepancies in the GRACE time series can be detected for Feb 2015

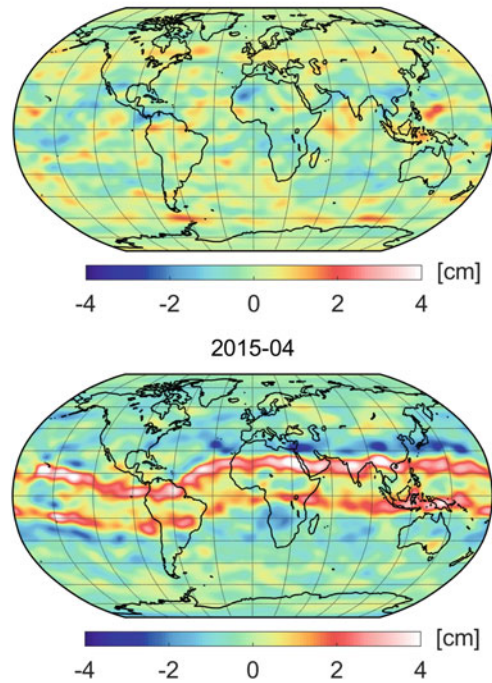


Fig. 3 Geoid height differences with respect to ITSG-Grace2018 of the GRACE GPS-based gravity field solutions for Aug 2014 (*top*) and Apr 2015 (*bottom*). Gaussian smoothing with a 500 km radius is applied

and Oct 2016. In both cases, the degradation of the monthly solutions can be explained by a sparse ground track coverage due to periods of near repeat orbits. Although it might be expected that only higher degrees suffer from spatial coverage problems, difference degree amplitudes for Feb 2015, as show in Fig. 4 (top), illustrate that the impact strongly depends on the maximum degree used for the gravity field

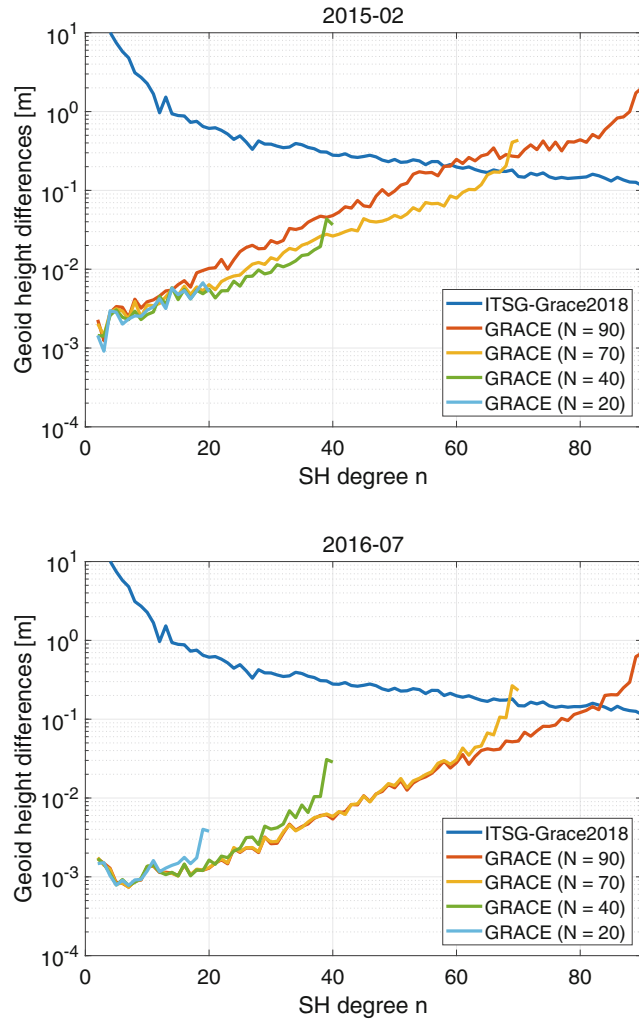


Fig. 4 Difference degree amplitudes in terms of geoid heights with respect to ITSG-Grace2018 for GRACE GPS-based gravity field solutions with different values for the maximum degree $N \in \{90, 70, 40, 20\}$ in the case of Feb 2015 (top) and Jul 2016 (bottom)

estimation. With an increasing maximum degree, the quality of the solutions decreases, demonstrating a high correlation between higher and lower degree coefficients. However, as shown in Fig. 4 (bottom), solutions with a lower maximum degree reveal large omission errors in the case of a nominal month like Jul 2016. Moreover, it should be noted that the plotted solutions with a lower maximum degree (e.g., 20 or 40) still require the use of a higher degree a priori gravity field to obtain a sufficiently accurate initial orbit determination. This inconsistency in the maximum degree might introduce a priori knowledge to the estimation (as mentioned in Sect. 1).

Similar to GRACE, the difference degree amplitudes of the Swarm time series shown in Fig. 2 (bottom) also reveal a limited performance in the early mission phase, mainly related to non-optimal settings of the GPS receivers (cf. van den IJssel et al. 2016). Starting in May 2015, the

quality of the Swarm time series substantially improves when several modifications of the GPS tracking loop bandwidths have been performed (Dahle et al. 2017). The benefit is most impressively visible for the relevant degrees below 20.

In comparison to the GRACE-FO time series (Fig. 2, top right), the Swarm solutions are of superior quality, which is also reflected when plotting the ratio of both time series (not shown). This again is consistent with differences in the satellites' altitudes (cf. Fig. 1). Beginning in Feb 2020, a degradation can be identified in both GPS-based gravity field time series. While for Swarm it is only slightly visible in the lower degrees, this behavior is more pronounced in the case of GRACE-FO, where apparently all degrees are affected. The appearance of this effect coincides with the activation of a new flex power mode for various GPS satellites in Feb 2020 that allows to redistribute the transmit power between different signal components (cf. Steigenberger et al. 2019). As also reported by Huang et al. (2022), this causes problems with some LEO GPS receivers (e.g., GRACE-FO), resulting in a slightly degraded quality of the orbit and gravity field solutions in this study.

4 Combination of Gravity Field Time Series

In the framework of COST-G, monthly gravity field time series are operationally combined to provide consolidated and improved products (Jäggi et al. 2020). Solutions from different institutes (analysis centers) are combined based on data of a single LEO mission, e.g., solutions based on K-band data from GRACE/-FO or GPS data from Swarm. The gravity field combination can either be done at solution or NEQ level, where the latter case benefits from taking into account the full correlations between the estimated parameter. However, as outlined in Teixeira da Encarnação and Visser (2019), a robust NEQ level combination is based on the assumption of equivalent information content of all NEQs. In the above described combination scenario (single LEO mission, multi-institutional approach), heterogeneous processing and error modeling strategies make it necessary to introduce empirical factors to balance the impact of the individual NEQs (cf. Meyer et al. 2019). But even following such a procedure, Teixeira da Encarnação et al. (2020) reported that a combination of Swarm GPS-based gravity field models at solution level provides a better agreement to GRACE K-band data than a combination at NEQ level.

In the scenario of this study (multi-LEO mission, single approach), we are confronted with similar issues, as the individual gravity field solutions differ in their signal content and sensitivity, e.g., due to differences in the orbital altitude or the sampling rate of the kinematic positions. Thus, to simplify the analysis in a first step, the focus of this paper

is confined to the combination of gravity field time series at solution level. In the following, the performance of two combination strategies is studied: (i) a VCE approach using monthly relative field-wise weights, and (ii) a “stochastic” combination that takes into account the standard deviations (formal errors) of the SH coefficients. Both combination strategies are briefly introduced in the following and applied to the individual satellite solutions.

4.1 VCE Combination

Based on iterative least-squares VCE (Teunissen and Amiri-Simkooei 2008) as frequently used for stacking of NEQs, Jean et al. (2018) introduced a VCE approach at solution level that is applied for the COST-G combination. Following Meyer et al. (2019), the gravity field coefficients of the individual solutions are used as pseudo-observations (i.e., the design, weight and normal matrix all become identity matrices) to iteratively derive monthly field-wise weights.

Assuming there are N solutions with their SH coefficients $x_{nm}^i \in \{C_{nm}^i, S_{nm}^i\}, i = 1, \dots, N$, where n and m are the SH degree and order, the weighted combination in an iteration step k is defined by

$$\hat{x}_{nm}^{(k)} = \frac{1}{\sum_{i=1}^N w^{i,k}} \sum_{i=1}^N w^{i,k} x_{nm}^i, \quad (1)$$

where $w^{i,k}$ denotes the weight of solution i in iteration step k . Starting with equal weights $w^{i,0} = 1/N$ for each solution, the weights in iteration k are given by

$$w^{i,k} = \left(1 - \frac{w^{i,k-1}}{\sum_{i=1}^N w^{i,k-1}}\right) \left[\text{RMS} \left(x_{nm}^i - \hat{x}_{nm}^{(k-1)} \right) \right]^{-2}, \quad (2)$$

where RMS is the root-mean-square value.

For the estimation of VCE weights, we analyzed to which maximum degree the SH coefficients should be introduced to Eq. (2), e.g., degree 70, 40, or 20. Similar to findings in Teixeira da Encarnação et al. (2020), it turned out that the used maximum degree needs to be restricted to prevent that VCE weights are strongly dominated by the noise of the higher degrees. A comparison of VCE combinations based on weights derived from SH coefficients up to degree 20 and 40 reveals a slightly better performance for degree 40 in terms of estimated mass trends and variations (Sect. 5).

For the case where SH coefficients up to degree 40 are taken into account, Fig. 5 presents the resulting monthly VCE weights after four iteration steps, where a sufficient convergence level is reached (cf. Meyer et al. 2019). The overall differences reflected in the weights are clearly correlated with the different orbital altitudes of the LEO satellites

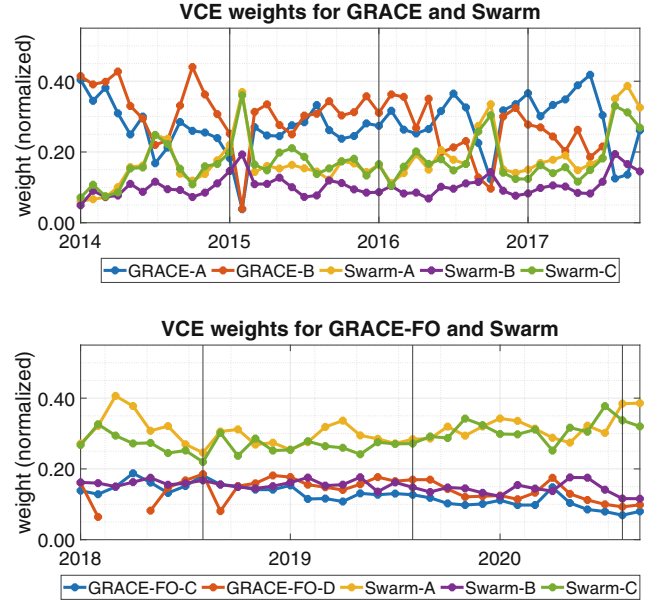


Fig. 5 Monthly field-wise weights derived from VCE (four iterations) based on the SH coefficients up to d/o 40 of the GPS-based gravity field solutions for the LEO satellites of the GRACE and Swarm missions between Jan 2014 and Oct 2017 (top), as well as the GRACE-FO and Swarm missions between Jun 2018 and Feb 2021 (bottom)

as plotted in Fig. 1. This might be explained as follows: satellites at lower altitudes obtain higher weights as they have a higher sensitivity to the Earth’s gravity field with a lower noise level. However, satellites at lower altitudes are generally more affected by ionospheric disturbances that influence the quality of the gravity field recovery, see, e.g., Fig. 2 in the case of GRACE. In this regard, the VCE weights seems to be less sensitive as only in a few months, where the GRACE solution suffers from severe problems like the near repeat orbits in Feb 2015 and Oct 2016, the sequence significantly changes.

4.2 Stochastic Combination

In the case of the stochastic combination, the SH coefficients x_{nm}^i of the individual solutions are combined based on their respective standard deviations $\sigma_{x_{nm}^i}$ obtained from the least-squares adjustment. Generalized from the formulas presented in Huang and Véronneau (2013), monthly coefficient-wise weights are determined by

$$w_{nm}^i = \frac{1}{\sum_{i=1}^N (\sigma_{x_{nm}^i})^2} \sum_{\substack{j=1, \dots, N \\ j \neq i}} (\sigma_{x_{nm}^j})^2. \quad (3)$$

As the standard deviations $\sigma_{x_{nm}^i}$ depend on the number of observations, differences in the sampling rates of the kinematic positions (see Table 1) need to be compensated. To this end, the increased sampling rate of the Swarm kinematic

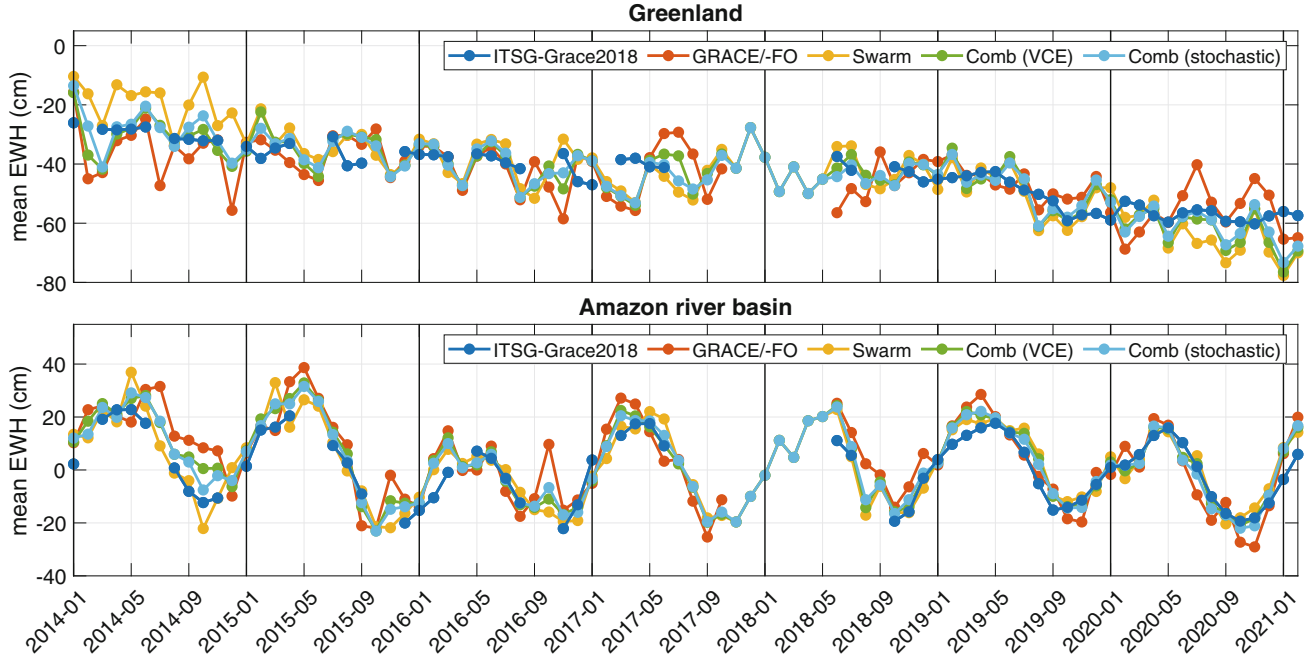


Fig. 6 Time-variable gravity field signal (up to d/o 20) of the Greenland ice sheet (*top*) and the Amazon river basin (*bottom*) recovered from GRACE, GRACE-FO and Swarm kinematic positions and combina-

tions thereof in comparison to ITSG-Grace2018. Gaussian smoothing with a 500 km radius is applied

positions from 10 to 5 s is considered by applying a factor of $\sqrt{2}$ to the standard deviations of the Swarm solutions starting from Jul 2014. The weighted combination is then defined by

$$\hat{x}_{nm} = \frac{1}{\sum_{i=1}^N w_{nm}^i} \sum_{i=1}^N w_{nm}^i x_{nm}^i. \quad (4)$$

5 Evaluation of Mass Trends and Variations

In this section, we use the monthly GPS-based gravity field solutions and their combinations to recover time-variable mass trends and variations. For this purpose, we analyze time series of mean equivalent water height (EWH) values over the Greenland ice sheet (area: $\sim 2.07 \times 10^6 \text{ km}^2$) and the Amazon river basin (area: $\sim 6.21 \times 10^6 \text{ km}^2$), regions with strong ice mass loss or high hydrology-induced seasonal variations. For assessment, a time series derived from monthly ITSG-Grace2018 solutions will serve as a superior reference.

The time series are derived as follows: (i) monthly SH coefficients are transformed to EWH (Wahr et al. 1998), subtracted by the signal of GOCO06s (Kvas et al. 2021) to remove the static gravity field part, and smoothed by a 500 km Gaussian filter, (ii) for each month, these SH coefficients are evaluated up to d/o 20 to compute EWH values on a regular $0.5^\circ \times 0.5^\circ$ grid covering the selected regions, (iii) values are averaged over these regions to derive

Table 2 RMS differences (cm) of GPS-based gravity field time series and their combinations with respect to ITSG-Grace2018 for Greenland and the Amazon river basin for Jan 2014 – Jun 2017 (T_1) and Jun 2018 – Feb 2021 (T_2). For comparison, values are also shown for a combination using the arithmetic average of the SH coefficients

	Greenland		Amazon	
	T_1	T_2	T_1	T_2
GRACE/-FO	8.23	8.07	9.95	7.70
Swarm	9.23	8.35	6.61	5.26
Comb (VCE)	7.40	7.18	7.14	5.11
Comb (stochastic)	7.06	6.43	6.15	5.23
Comb (average)	7.15	6.17	6.29	5.37

monthly area-weighted mean EWH estimates (i.e., weighted by the cosine of the latitude of the grid cells).

In Fig. 6, the time series of mean EWH values derived from the LEO gravity field solutions and combinations thereof are displayed and compared to ITSG-Grace2018. Results are shown for the Greenland ice sheet and the Amazon river basin at the top and bottom of Fig. 6, respectively. To quantify the performance of the time series, Table 2 provides RMS differences of their mean EWH values with respect to ITSG-Grace2018. For this purpose, the time series is split into two time spans, T_1 (Jan 2014–Jun 2017) and T_2 (Jun 2018–Feb 2021), representing the GRACE and GRACE-FO mission periods, respectively. Note that values in Table 2 are based solely on months with available ITSG-Grace2018 solutions, i.e., 31 months in each time span.

In the case of Greenland (Fig. 6, top), the mass loss represented by the ITSG-Grace2018 time series (blue curve) decreases from about -20 to -60 cm between 2014 and 2021, showing some smaller seasonal variations. Although the GPS-derived time series of GRACE/-FO (red curve) and Swarm (yellow curve) have a larger scatter, they provide a remarkably good long-term agreement with the K-band solution. At the beginning of the time span, the GRACE and Swarm solutions exhibit some larger discrepancies. The mean EWH values derived from Swarm are systematically larger than those of ITSG-Grace2018, which can be attributed to the problems in the early mission phase pointed out in Sect. 3. In contrast, the GRACE time series tends to produce smaller values than ITSG-Grace2018 in this period. Here, larger amplitudes follow a certain periodicity that is related to the 161-day cycle when the β angle of the GRACE orbit is crossing zero (β : angle between the orbital plane and the Earth-Sun direction). For these periods (e.g., in Feb, Jul, Dec in the case of 2014), it is known that the recovery of the C_{20} coefficient is affected in GRACE GPS and K-band solutions (Cheng and Ries 2017). However, in contrast to gaps in the K-band time series (mainly due to instrument shut-downs in these periods), the derived GRACE GPS-only time series is uninterrupted.

The benefit of a continuous time series can also be highlighted for the gap between GRACE and GRACE-FO, where GRACE GPS data can provide four additional monthly solutions at the end of the mission. This can be of particular interest as during the GRACE/-FO gap in 2017 and 2018, the ice mass loss trend in Greenland is significantly attenuated (cf. Sasgen et al. 2020). This temporary phenomenon is reflected by a roughly constant mean EWH value in the GPS-based times series of GRACE, and particularly Swarm.

While the RMS differences in Table 2 demonstrate that the GRACE time series is more consistent to the ITSG-Grace2018 signal in the time period T_1 (8.23 cm compared to 9.23 cm for Swarm), the GPS-based GRACE-FO and Swarm time series achieve comparable results in period T_2 , both obtaining RMS differences at a lower 8 cm-level. Here it is noticeable that starting with 2020 (when GPS flex power was activated), the scatter in the GRACE-FO time series significantly increases and the Swarm time series tends to gradually drift away from the ITSG-Grace2018 signal.

For the Amazon river basin (Fig. 6, bottom), the time-variable gravity signal of ITSG-Grace2018 shows strong seasonal variations between ± 20 cm, where maximum and minimum values are reached in spring and autumn, respectively. Compared to Greenland, the GPS-based LEO time series for the Amazon river basin are generally more consistent to ITSG-Grace2018, particularly in the case of Swarm, where RMS differences are significantly smaller (up to 37 % in time period T_2 , see Table 2). This can certainly be explained by the approximately three times larger area compared to

Greenland, where potential discrepancies in the EWH values average out to a larger extent. The only exception is the performance of the GRACE time series in T_1 , attaining a large RMS difference of ~ 10 cm.

Mostly at the beginning of the time span T_1 , the Swarm and particularly the GRACE time series tend to over- or underestimate the peaks of the seasonal variations. Moreover, two prominent outliers are visible in the GRACE time series, in Nov 2015 and Oct 2016, where in the latter case the gravity field signal is impaired due to coverage problems in this month. During the first months of the GRACE/-FO data gap, when K-band data was unavailable but GPS data was still being collected, both LEO time series match quite well and produce a reasonable signal. While the GRACE-FO time series shows slightly larger amplitudes in the seasonal peaks, the Swarm time series is remarkably consistent to the ITSG-Grace2018 signal for the time period T_2 , which is also indicated by the small RMS difference of 5.26 cm in Table 2.

The combined LEO gravity field time series are plotted by the green and light-blue curves in Fig. 6. Generally, it can be seen that both combinations are able to reduce the scatter around the ITSG-Grace2018 signal (e.g., in 2014 for Greenland) and effectively compensate for outliers of the individual solutions (e.g., in Oct 2016 for the Amazon river basin). The improved performance is also reflected by reduced RMS values in Table 2. In the case of Greenland, a decrease in the RMS differences of up to 11 % and 20 % can be detected for the VCE and stochastic combination, respectively, relative to the best individual time series. Due to the generally good performance of the Swarm time series in the case of the Amazon river basin, the additional value for a combination with the GRACE and GRACE-FO solutions is limited. Therefore, as visible from Table 2, improvements in the RMS differences with respect to the Swarm time series are confined to a maximum reduction of 3 % and 7 % for the VCE and stochastic combination, respectively.

In total, both combination strategies achieve comparable results with a preference for the stochastic combination that provides smaller residuals to ITSG-Grace2018 in 52 % (Greenland) and 58 % (Amazon river basin) of the months and outperforms the VCE combination in terms of RMS differences (except for T_2 in the latter case). For comparison, Table 2 also provides RMS differences for a combination based on the arithmetic average of the SH coefficients. In the time span T_1 its performance is in between the analyzed combinations, while in T_2 the RMS difference is about 4 % smaller (Greenland) or 2 % larger (Amazon river basin) compared to the stochastic combination.

One of the most noticeable differences between the time series of the VCE and stochastic combinations can be seen for the Amazon river basin in Oct 2014. For this month, Fig. 7 shows the gridded EWH residuals of the different solutions

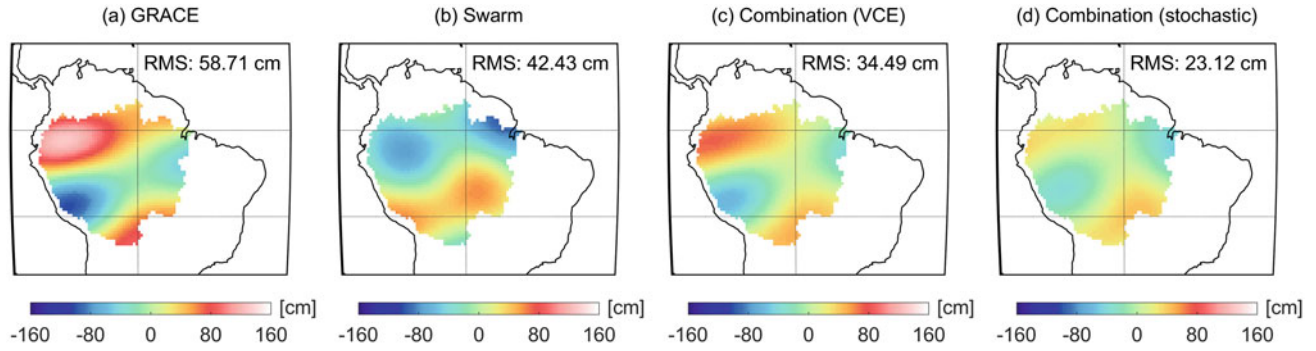


Fig. 7 Equivalent water height differences (up to d/o 20) with respect to ITSG-Grace2018 of (a) GRACE and (b) Swarm GPS-based gravity field solution as well as their (c) VCE and (d) stochastic combination for Oct 2014 in the Amazon river basin. Gaussian smoothing with a 500 km

radius is applied. Additionally, for each solution the area-weighted RMS of the differences is specified, i.e., weighted by the cosine of the latitude

with respect to ITSG-Grace2018. Here, the GRACE-derived values reveal strong positive anomalies in the northern and southern part of the Amazon river basin, resulting in the high mean EWH value displayed in Fig. 6. Both of these anomalies are related to ionospheric-induced artifacts along the geomagnetic equator (cf. Fig. 3). In contrast, the Swarm solution is far less affected by the ionosphere, but also shows stronger positive and negative differences in the south and north of the Amazon river basin, respectively.

Concerning the combinations, it can be seen that they are both able to reduce the disturbances of the individual solutions. However, the VCE combination is apparently more driven by the GRACE solution as can be seen by the considerably large remaining residuals in the north of the Amazon river basin. This dominance of the GRACE solution can be seen as a consequence of the strong impact of the orbital altitudes on the VCE weights as shown in Fig. 5. Thus, this example illustrates the disadvantage of the VCE combination approach when using inhomogeneous data from different LEO satellites. In contrast, the stochastic combination is capable to strongly attenuate the anomalies originating from the GRACE and Swarm solutions. In terms of weighted RMS values with respect to ITSG-Grace2018, the stochastic combination provides a 30 % smaller value, underlining that this procedure is more robust against outliers.

6 Conclusions and Outlook

In this paper, we use GPS-based kinematic LEO orbit positions of the GRACE, GRACE-FO and Swarm missions to recover time-variable gravity field signals. By studying mass variations in Greenland and the Amazon river basin, the GPS-based gravity field time series are in good agreement with those derived from inter-satellite ranging and are able to fill gaps reasonably at spatial scales of about 1000 km

(d/o 20). Moreover, it was demonstrated that a combination of the time series provides a further improved estimation of time-variable signals, indicated by a reduction of RMS differences by $\sim 10\%$ to 20% with respect to a inter-satellite ranging solution. Here, it can be pointed out that the VCE combination at solution level as applied for COST-G is of limited use for a multi-mission scenario, as derived weights are mainly driven by the different altitudes of the LEOs. This might be related to the used simple case where the normal matrix is equal to the identity matrix, which cannot properly reflect differences in the geometry of LEO missions. In comparison, a combination that takes into account the standard deviations (formal errors) of the gravity field coefficients, turned out to cope better with this setting and underlines the importance of a degree-dependent weighting.

As a next step, we aim to extend our monthly GRACE/-FO time series and include gravity field information derived from additional LEO satellites, e.g., from the Sentinel constellation. Further improvements of the current GRACE time series can be expected by a refinement of the used kinematic orbits, e.g., considering measures to mitigate the influence of ionospheric disturbances would be beneficial for the years 2014 and 2015. Beside a classical screening as currently done for the operational Swarm orbits, advanced weighting techniques might also be considered (cf. Schreiter et al. 2019) that have demonstrated their advantage, e.g., in the GOCE GPS-based gravity field recovery (Grombein et al. 2019). Finally, we will focus on the combination of the GPS-based gravity field time series at normal equation level.

Acknowledgements The authors would like to acknowledge two anonymous reviewers for their comments, which helped to improve the manuscript. This research was supported by the European Research Council under the grant agreement no. 817919 (project SPACE TIE). All views expressed are those of the authors and not of the European Research Council. Calculations in this study were performed on UBE-LIX, the HPC cluster at the University of Bern.

References

- Arnold D, Jäggi A (2020a) AIUB GRACE kinematic orbits, release 01. Astronomical Institute, University of Bern. <https://doi.org/10.48350/158372>
- Arnold D, Jäggi A (2020b) AIUB GRACE-FO kinematic orbits, release 01. Astronomical Institute, University of Bern. <https://doi.org/10.7892/boris.147231>
- Arnold D, Jäggi A (2021) AIUB Swarm kinematic orbits, release 03. Astronomical Institute, University of Bern. <https://doi.org/10.48350/158373>
- Baur O, et al. (2014) Comparison of GOCE-GPS gravity fields derived by different approaches. *J Geod* 88(10):959–973. <https://doi.org/10.1007/s00190-014-0736-6>
- Beutler G, Jäggi A, Mervart L, Meyer U (2010) The celestial mechanics approach: theoretical foundations. *J Geod* 84(10):605–624. <https://doi.org/10.1007/s00190-010-0401-7>
- Bock H, Dach R, Jäggi A, Beutler G (2009) High-rate GPS clock corrections from CODE: support of 1 Hz applications. *J Geod* 83(11):1083–1094. <https://doi.org/10.1007/s00190-009-0326-1>
- Cheng M, Ries J (2017) The unexpected signal in GRACE estimates of C_{20} . *J Geod* 91(8):897–914. <https://doi.org/10.1007/s00190-016-0995-5>
- Dach R, et al. (2009) GNSS processing at CODE: status report. *J Geod* 83(3–4):353–365. <https://doi.org/10.1007/s00190-008-0281-2>
- Dach R, Lutz S, Walser P, Fridez P (eds) (2015) Bernese GNSS Software Version 5.2, Documentation. Astronomical Institute, University of Bern. <https://doi.org/10.7892/boris.72297>
- Dahle C, Arnold D, Jäggi A (2017) Impact of tracking loop settings of the Swarm GPS receiver on gravity field recovery. *Adv Space Res* 59(12):2843–2854. <https://doi.org/10.1016/j.asr.2017.03.003>
- Friis-Christensen E, Lühr H, Knudsen D, Haagmans R (2008) Swarm – an Earth observation mission investigating geospace. *Adv Space Res* 41(1):210–216. <https://doi.org/10.1016/j.asr.2006.10.008>
- Grombein T, Arnold D, Jäggi A (2019) GPS-based gravity field recovery from reprocessed GOCE precise science orbits. In: *Geophys Res Abstr vol 21, EGU 2019, Vienna*. <https://doi.org/10.7892/boris.143198>
- Grombein T, Arnold D, Jäggi A (2021) Time-variable gravity field recovery from reprocessed GOCE precise science orbits. 43rd COSPAR SA, Sydney. <https://doi.org/10.48350/152967>
- Guo X, Ditmar P, Zhao Q, Xiao Y (2020) Improved recovery of temporal variations of the Earth's gravity field from satellite kinematic orbits using an epoch-difference scheme. *J Geod* 94(8):69. <https://doi.org/10.1007/s00190-020-01392-6>
- Huang J, Véronneau M (2013) Canadian gravimetric geoid model 2010. *J Geod* 87(8):771–790. <https://doi.org/10.1007/s00190-013-0645-0>
- Huang W, et al. (2022) Estimation of GPS transmitter antenna phase center offsets by integrating space-based GPS observations. *Adv Space Res* 69(7):2682–2696. <https://doi.org/10.1016/j.asr.2022.01.004>
- Jäggi A, Hugentobler U, Beutler G (2006) Pseudo-stochastic orbit modeling techniques for low-Earth orbiters. *J Geod* 80(1):47–60. <https://doi.org/10.1007/s00190-006-0029-9>
- Jäggi A, et al. (2009) Phase center modeling for LEO GPS receiver antennas and its impact on precise orbit determination. *J Geod* 83(12):1145–1162. <https://doi.org/10.1007/s00190-009-0333-2>
- Jäggi A, Bock H, Meyer U, Beutler G, van den IJssel J (2015) GOCE: assessment of GPS-only gravity field determination. *J Geod* 89(1):33–48. <https://doi.org/10.1007/s00190-014-0759-z>
- Jäggi A, et al. (2016) Swarm kinematic orbits and gravity fields from 18 months of GPS data. *Adv Space Res* 57(1):218–233. <https://doi.org/10.1016/j.asr.2015.10.035>
- Jäggi A, et al. (2020) International combination service for time-variable gravity fields – Start of operational phase and future perspectives. In: *IAG Symp*. https://doi.org/10.1007/1345_2020_109
- Jean Y, Meyer U, Jäggi A (2018) Combination of GRACE monthly gravity field solutions from different processing strategies. *J Geod* 92(11):1313–1328. <https://doi.org/10.1007/s00190-018-1123-5>
- Kvas A, et al. (2019) ITSG-Grace2018: overview and evaluation of a new GRACE-only gravity field time series. *J Geophys Res* 124(8):9332–9344. <https://doi.org/10.1029/2019JB017415>
- Kvas A, et al. (2021) GOCO06s – a satellite-only global gravity field model. *Earth Syst Sci Data* 13(1):99–118. <https://doi.org/10.5194/essd-13-99-2021>
- Landerer FW, et al. (2020) Extending the global mass change data record: GRACE Follow-On instrument and science data performance. *Geophys Res Lett* 47(12):e2020GL088306. <https://doi.org/10.1029/2020GL088306>
- Meyer U, Jäggi A, Beutler G, Bock H (2015) The impact of common versus separate estimation of orbit parameters on GRACE gravity field. *J Geod* 89(7):685–696. <https://doi.org/10.1007/s00190-015-0807-3>
- Meyer U, et al. (2019) Combination of GRACE monthly gravity fields on the normal equation level. *J Geod* 93(9):1645–1658. <https://doi.org/10.1007/s00190-019-01274-6>
- Richter H, et al. (2021) Reconstructing GRACE-type time-variable gravity from the Swarm satellites. *Sci Rep* 11(2):1117. <https://doi.org/10.1038/s41598-020-80752-w>
- Sasgen I, et al. (2020) Return to rapid ice loss in Greenland and record loss in 2019 detected by the GRACE-FO satellites. *Commun Earth Environ* 1(8). <https://doi.org/10.1038/s43247-020-0010-1>
- Schaer S, et al. (2021) The CODE ambiguity-fixed clock and phase bias analysis products: generation, properties, and performance. *J Geod* 95(7):81. <https://doi.org/10.1007/s00190-021-01521-9>
- Schreiter L, Arnold D, Sterken V, Jäggi A (2019) Mitigation of ionospheric signatures in Swarm GPS gravity field estimation using weighting strategies. *Ann Geophys* 37(1):111–127. <https://doi.org/10.5194/angeo-37-111-2019>
- Steigenberger P, Thörlert S, Montenbruck O (2019) Flex power on GPS Block IIR-M and IIF. *GPS Solut* 23(1):8. <https://doi.org/10.1007/s10291-018-0797-8>
- Švehla D, Rothacher M (2005) Kinematic precise orbit determination for gravity field determination. In: *IAG Symp* 128, pp 181–188. https://doi.org/10.1007/3-540-27432-4_32
- Tapley BD, Bettadpur S, Watkins M, Reigber C (2004) The gravity recovery and climate experiment: Mission overview and early results. *Geophys Res Lett* 31(9):L09607. <https://doi.org/10.1029/2004GL019920>
- Teixeira da Encarnação J, Visser P (2019) TN-03: Swarm models validation. <https://doi.org/10.13140/RG.2.2.33313.76640>
- Teixeira da Encarnação J, et al. (2020) Description of the multi-approach gravity field models from Swarm GPS data. *Earth Syst Sci Data* 12(2):1385–1417. <https://doi.org/10.5194/essd-12-1385-2020>
- Teunissen PJ, Amiri-Simkooei A (2008) Least-squares variance component estimation. *J Geod* 82(2):65–82. <https://doi.org/10.1007/s00190-007-0157-x>
- van den IJssel J, Forte B, Montenbruck O (2016) Impact of Swarm GPS receiver updates on POD performance. *Earth Planets Space* 68(1):85. <https://doi.org/10.1186/s40623-016-0459-4>
- Wahr J, Molenaar M, Bryan F (1998) Time variability of the Earth's gravity field: hydrological and oceanic effects and their possible detection using GRACE. *J Geophys Res* 103(B12):30205–30229. <https://doi.org/10.1029/98JB02844>
- Weigelt M, et al. (2013) Time-variable gravity signal in Greenland revealed by high-low satellite-to-satellite tracking. *J Geophys Res* 118(7):3848–3859. <https://doi.org/10.1002/jgrb.50283>
- Zhong L, Sónica K, Weigelt M, Liu B, Zou X (2021) Time-variable gravity field from the combination of HLSST and SLR. *Remote Sens* 13(17):3491. <https://doi.org/10.3390/rs13173491>

Open Access This chapter is licensed under the terms of the Creative Commons Attribution 4.0 International License (<http://creativecommons.org/licenses/by/4.0/>), which permits use, sharing, adaptation, distribution and reproduction in any medium or format, as long as you give appropriate credit to the original author(s) and the source, provide a link to the Creative Commons license and indicate if changes were made.

The images or other third party material in this chapter are included in the chapter's Creative Commons license, unless indicated otherwise in a credit line to the material. If material is not included in the chapter's Creative Commons license and your intended use is not permitted by statutory regulation or exceeds the permitted use, you will need to obtain permission directly from the copyright holder.

